Supplementary information to

Molecular Qubits Based on Nuclear–Spin–Free Nickel-Ions

Katharina Bader, Simon Schlindwein, Dietrich Gudat, Joris van Slageren

Index

1. Synthesis of Compounds and Samples

All chemicals and solvents were used as purchased without further purification.

1.1. Perdeuterotetraphenylphosphonium bromide, $(d_{20}\text{-}PPh_4)Br$

In a pressure cylinder, deuterated triphenylphosphine (1.0000 g, 3.6 mmol) was combined with anhydrous nickel(II)bromide (0.3933 g, 1.8 mmol) and deuterated phenylbromide (0.76 ml, 7.2 mmol). The pressure cylinder was sealed and heated to 180°C for three hours. After cooling, 50 ml of demineralized water was added to the blue-green solid. After stirring for 15 min at 75°C, an aqueous blue solution and a fawn precipitate formed. The mixture was cooled in an ice bath and extracted with 3 x 50 ml of diethylether. The organic phase of the ether extraction was discarded and the aqueous phase was extracted with 3 x 50 ml chloroform. Subsequently, the solvent of the organic phase was removed and the resulting white solid was dried under reduced pressure. ^{13}C NMR (500MHz): 135.41 (t), 133.96 (td), 130.82 (td), 117.56, 116.85 ppm.

1.2. Ni-mnt^{dia,prot}: Bis-(tetraphenylphosphonium)-bis-(maleonitriledithiolato)nickelate(II), $(PPh_4)_2[Ni(mnt)_2]$

Sodium maleonitriledithiolate (279 mg, 1.5 mmol) was dissolved in 5 ml ethanol and 2 ml demineralized water. Subsequently nickel chloride hexahydrate (178 mg, 0.75 mmol), dissolved in 5 ml ethanol, and tetraphenylphosphonium bromide (629 mg, 1.50 mmol), dissolved in 15 ml ethanol were added under stirring. The red product precipitated immediately and was separated from the solution after 5 min by vacuum filtration. Washing of the product with 3 x 5 ml ethanol and drying for 20 h under reduced pressure gave a yield of 650 mg (85 % based on Ni). Elemental analysis: found (calcd) for $C_{56}H_{40}NiN_4P_2S_4$: C: 65.73 (66.08), H: 3.95 (3.96), N: 5.46 (5.50), S: 12.79 (12.60). UV/VIS (MeCN): λ_{max} in nm: 474, 379, 315, 270. IR (KBr-pellet): $\tilde{\nu}$ in cm^{-1} and assignment in brackets: 2196 ($\nu_{C\equiv N}$), 1479 ($\nu_{C=C}$).

1.3. Ni-mnt^{dia}: Bis-(Perdeutero-tetraphenylphos-phonium)-bis-(maleonitriledithiolato)nickelate(II), $(d_{20}\text{-}PPh_4)_2[Ni(mnt)_2]$

The same procedure as described above for **Ni-mnt^{dia,prot}** was performed, using a fifth of the amount of substances as indicated above and replacing PPh_4Br by perdeutero-tetraphenylphosphonium bromide (132 mg, 0.3 mmol). The dried compound was isolated with a yield of 118 mg (74 % based on Ni). Elemental analysis: found (calcd.) for $C_{56}D_{40}NiN_4P_2S_4$: C: 63.43 (63.57), H: 7.696 (7.610), N: 5.27 (5.30), S: 12.77 (12.12). UV/VIS in DCM: λ_{max} in nm: 481, 384, 318, 272, 229. IR (KBr-pellet): $\tilde{\nu}$ in cm^{-1} and assignment in brackets: 2195 ($\nu_{C\equiv N}$), 1479 ($\nu_{C=C}$).

1.4. Ni-mnt^{prot}: Tetraphenylphosphonium-bis-(maleonitriledithiolato)-nickelate(III), $(PPh_4)[Ni(mnt)_2]$

In a round flask, 150 mg of **Ni-mnt^{dia,prot}** (0.15 mmol) was dissolved in 5 ml acetonitrile. A solution of 45 mg iodine (0.18 mmol) in 1.5 ml methanol was added dropwise under stirring. The formed grey, fluffy precipitate was filtered and washed subsequently with 5 ml of methanol, demineralized water and diethylether. The crude product was re-precipitated three times from ice cold acetone/pentane (1:3) and finally recrystallized from acetone. The final product contains PPh_4I as side-product. Elemental analysis: found (calcd.) for $C_{32}H_{20}NiN_4PS_4$: C: 56.65 (57.46), H: 3.622 (2.970), N: 6.74 (8.26), S: 15.57 (18.90). UV/VIS in DCM: λ_{max} in nm: 866, 606, 481, 349 (sh), 314, 272, 237. IR (KBr-pellet): $\tilde{\nu}$ in cm^{-1} and assignment in brackets: 2205 ($\nu_{C\equiv N}$), 1436 ($\nu_{C=C}$).

1.5. Synthesis of Ni-mnt: Perdeutero-tetraphenylphosphonium-bis-(maleonitriledithiolato)nickelate(III), (d_{20}-PPh_4)[Ni(mnt)$_2$]

The same procedure as for the protonated analogue **Ni-mnt^{prot}** was applied, using 156 mg of **Ni-mnt^{dia}** (0.15 mmol) as starting material. The final product contains PPh_4I as side-product. Elemental analysis: found (calcd.) for $C_{32}D_{20}NiN_4PS_4$: C: 54.18 (55.02), H: 2.93 (5.77), N: 7.33 (8.02), S: 17.03 (18.36). UV/VIS in DCM: λ_{max} in nm: 866, 606, 481, 349 (sh), 314, 272, 237. IR (KBr-pellet): $\tilde{\nu}$ in cm^{-1} and assignment in brackets: 2205 ($\nu_{C\equiv N}$), 1436 ($\nu_{C=C}$).

1.6. Ni-dip: Triethylammonium-bis(3-(diphenylphosphoryl)-methyl-benzene-1,2-dithiolato)nickelat(II), ($HNEt_3$)[Ni(dip)$_2$]

The synthesis of this compound was accepted for publication in Inorganic Chemistry.[1]

1.7. Synthesis of doped powders Ni-mnt$_{0.01\%}$ and $\mathrm{Ni\text{-}mnt}^{\mathrm{prot}}_{0.01\%}$

Doped powders were obtained by dissolving the corresponding paramagnetic (**Ni-mnt**; **Ni-mnt^{prot}**) and diamagnetic compounds (**Ni-mnt^{dia}**; **Ni-mnt^{dia,prot}**) in the desired molar ratios (paramagnetic : diamagnetic = 0.01 : 99.99) in a minimum volume of acetone, and subsequent evaporation of the solvent under reduced pressure. The resulting powders were dried in vacuo and finely ground.

2. Pulsed Q-band Measurements on Ni-dip in Solution

Table S1: Simulation parameters for ESE-detected EPR spectra of **Ni-dip** in 1 mM solution (d_2-DCM/CS_2, 1 : 1) at 7 K.

g_z	g_y	g_x	*lwpp*	*gStrain*
2.1725 ± 0.0005	2.0405 ± 0.0005	2.0075 ± 0.0005	[0 0.8]	[0.007 0 0.02]

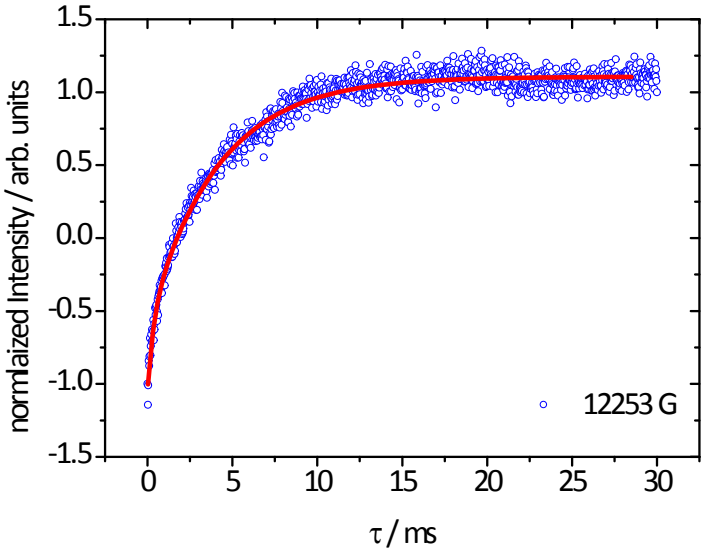

Figure S1: Inversion recovery measurement data (open symbols) and biexponential fits (solid lines) of **Ni-dip** in 1 mM solution (d_2-DCM/CS_2, 1 : 1) at 7 K and 12253 G. Fit parameters: A_f = -0.45 ± 0.04, $T_{1,f}$ = (0.33 ± 0.05) ms, A_s = -1.70 ± 0.02, $T_{1,s}$ = (4.05 ± 0.06) ms

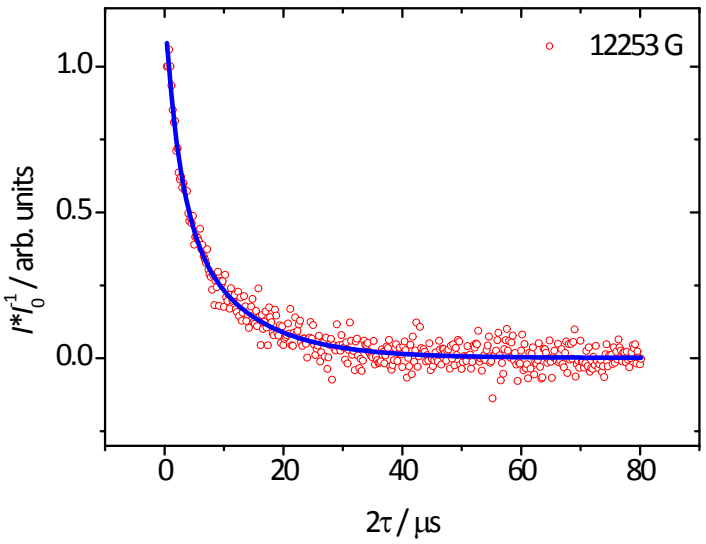

Figure S2: Hahn echo measurement data (open symbols) and biexponential fits (solid lines) of **Ni-dip** in 1 mM solution (d_2-DCM/CS_2, 1 : 1) at 7 K and 12253 G. Fit parameters: A_f = 0.64 ± 0.06, $T_{M,f}$ = (2.5 ± 0.4) µs, A_s = 0.56 ± 0.07, $T_{M,s}$ = (11 ± 1) µs.

3. Pulsed Q-band Measurements on Ni-mnt in Solution

Table S2: Simulation parameters for ESE-detected EPR spectra of **Ni-mnt** in 1 mM solution (d_2-DCM/CS_2, 1 : 1) at 7 K.

g_z	g_y	g_x	*lwpp*	*gStrain*
2.1390 ± 0.0005	2.0404 ± 0.0005	1.9935 ± 0.0005	[0 .6 0.1]	[0.005 0 0.015]

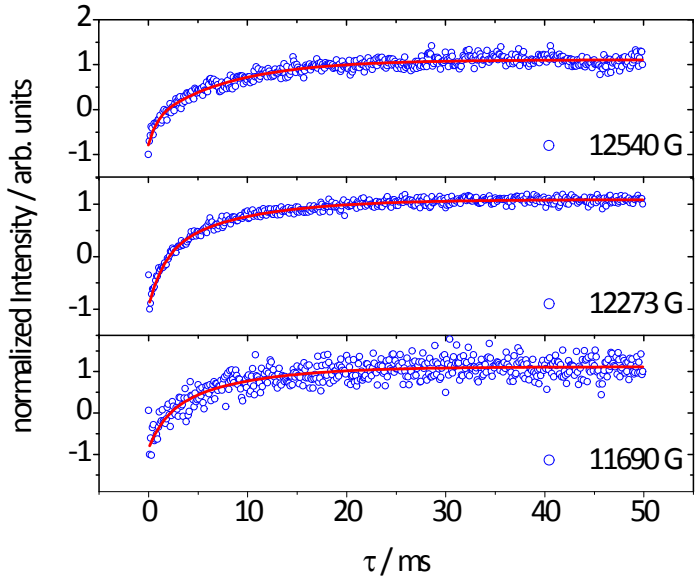

Figure S3: Inversion recovery measurement data (open symbols) and biexponential fits (solid lines) of **Ni-mnt** in 1 mM solution (d_2-DCM/CS_2, 1 : 1) at 7 K and different field positions as indicated. Fit parameters are given in Table 3.

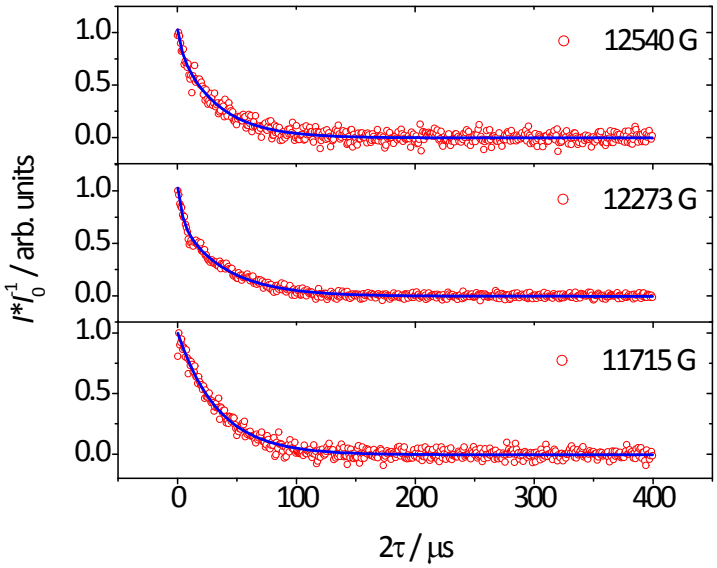

Figure S4: Hahn echo measurement data (open symbols) and biexponential fits (solid lines) of **Ni-mnt** in 1 mM solution (d_2-DCM/CS_2, 1 : 1) at 7 K and different field positions as indicated. Fit parameters are given in Table 4.

Table S3: Parameters of biexponential fit functions for inversion recovery experiments of **Ni-mnt** in 1 mM solution (d_2-DCM/CS_2, 1 : 1) at 7 K and different field positions as indicated.

B_0 / G	A_f	$T_{1,f}$ / ms	A_s	$T_{1,s}$ / ms
12540	-0.54 ± 0.07	0.8 ± 0.2	-1.36 ± 0.05	8.0 ± 0.4
12273	-0.99 ± 0.06	1.6 ± 0.2	-1.03 ± 0.06	8.5 ± 0.5
11690	-0.8 ± 0.3	1.7 ± 0.9	-1.2 ± 0.3	8 ± 2

Table S4: Parameters of biexponential fit functions for Hahn echo experiments of **Ni-mnt** in 1 mM solution (d_2-DCM/CS_2, 1 : 1) at 7 K and different field positions as indicated.

B_0 / G	A_f	$T_{M,f}$ / µs	A_s	$T_{M,s}$ / µs
12540	0.20 ± 0.05	4 ± 2	0.87 ± 0.03	33 ± 1
12273	0.34 ± 0.02	3.7 ± 0.5	0.74 ± 0.01	38.7 ± 0.08
11715	-	-	1.02 ± 0.01	34.2 ± 0.6

4. Pulsed Q-band Measurements on Ni-mnt in Doped Powders

4.1. $Ni - mnt_{0.01\%}$

4.1.1. ESE-detected Spectra

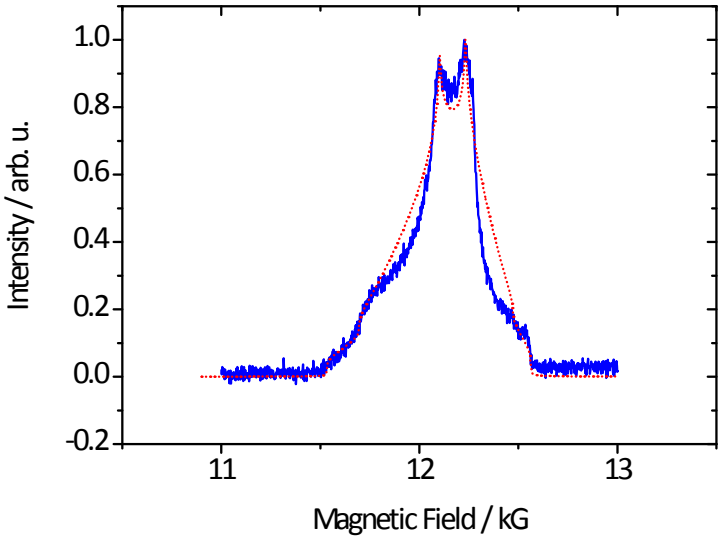

Figure S5: ESE detected EPR-spectrum of **Ni-mnt$_{0.01\%}$** at 7 K (blue, solid line) and simulation (red, broken line; parameters see Table 5).

Table S5: Simulation parameters for ESE-detected EPR spectra of **Ni-mnt$_{0.01\%}$** at 7 K. Two S = ½ spin systems were used in the simulation as well as a slight orientation effect with a preferential orientation of the molecules along the g_y-axis.

System	g_z	g_y	g_x	lwpp	weight
1	2.1980 ± 0.0005	2.0440 ± 0.0005	1.9905 ± 0.0005	[0.2 0.3]	1
2	2.1680 ± 0.0005	2.0660 ± 0.0005	2.0050 ± 0.0005	[0.2 0.3]	0.9

4.1.2. Orientation Dependence of Electron Spin Relaxation

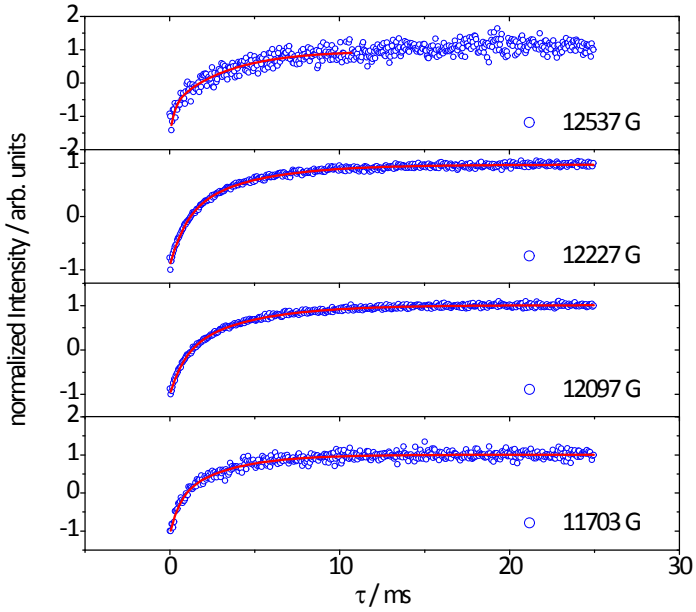

Figure S6: Inversion recovery measurement data (open symbols) and biexponential fits (solid lines) of **Ni-mnt$_{0.01\%}$** at 7 K and different field positions as indicated. Fit parameters are given in Table 6.

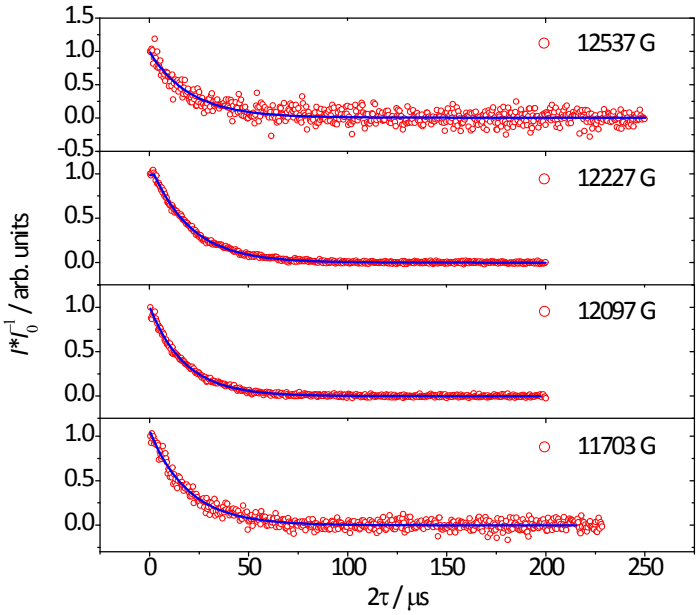

Figure S7: Hahn echo measurement data (open symbols) and biexponential fits (solid lines) of **Ni-mnt$_{0.01\%}$** at 7 K and different field positions as indicated. Fit parameters are given in Table 7.

Table S6: Parameters of biexponential fit functions for inversion recovery experiments of **Ni-mnt$_{0.01\%}$** at 7 K and different field positions as indicated.

B_0 / G	A_f	$T_{1,f}$ / ms	A_s	$T_{1,s}$ / ms
12537	-0.9 ± 0.3	0.3 ± 0.1	-1.67 ± 0.09	3.3 ± 0.4
12227	-0.91 ± 0.04	0.93 ± 0.06	-1.00 ± 0.05	4.0 ± 0.1
12097	-0.88 ± 0.04	0.85 ± 0.06	-1.13 ± 0.04	4.0 ± 0.1
11703	-0.89 ± 0.09	0.5 ± 0.1	-1.2 ± 0.09	3.0 ± 0.2

Table S7: Parameters of biexponential fit functions for Hahn echo experiments of **Ni-mnt$_{0.01\%}$** at 7 K and different field positions as indicated.

B_0 / G	A_s	$T_{M,s}$ / µs
12537	0.99 ± 0.03	20.5 ± 0.8
12227	1.109 ± 0.004	20.2 ± 0.1
12097	1.009 ± 0.004	17.8 ± 0.1
11703	1.06 ± 0.01	19.5 ± 0.4

4.1.3. Temperature Dependence of Electron Spin Relaxation

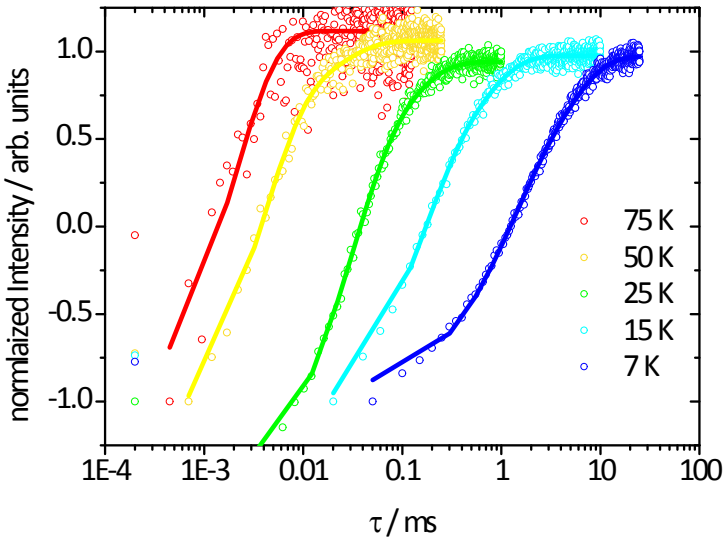

Figure S8: Inversion recovery data (open symbols) and mono-/biexponential fits (solid lines) of **Ni-mnt$_{0.01\%}$** measured at 12227 G, 7-100 K. Fit parameters are given in Table 8.

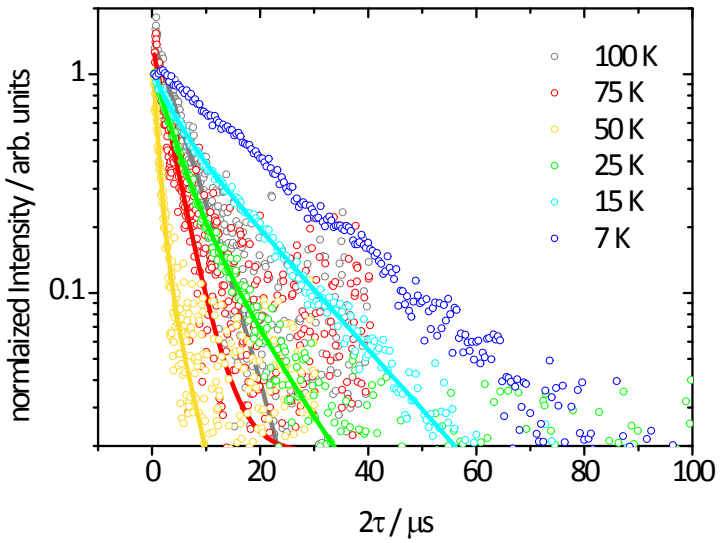

Figure S9: Hahn echo data (open circles) and bi-/monoexponential fit functions (solid lines) of **Ni-mnt$_{0.01\%}$** solution measured at Q-band, 12227 G, 7-100 K Fit parameters are given in Table 9.

Table S8: Parameters of bi-/monoexponential fit functions for inversion recovery experiments of **Ni-mnt$_{0.01\%}$** measured at 12227 G, 7-100 K.

T / K	A_f	$T_{1,f}$/ µs	A_s	$T_{1,s}$ / µs
7	-0.91 ± 0.04	927 ± 58	-0.99 ± 0.06	3986 ± 143
15	-1.34 ± 0.07	141 ± 11	-0.58 ± 0.04	580 ± 39
25	-1.83 ± 0.07	27 ± 1	-0.69 ± 0.07	105 ± 7
50	-1.97 ± 0.08	3.7 ± 0.3	-0.41 ± 0.08	21 ± 2
75	-2.3 ± 0.4	0.9 ± 0.3	-0.7 ± 0.3	5 ± 2

Table S9: Parameters of bi-/monoexponential fit functions for Hahn echo experiments of **Ni-mnt$_{0.01\%}$** measured at 12227 G, 7-100 K.

T / K	A_f	$T_{M,f}$/ µs	A_s	$T_{M,s}$ / µs
7	0.21 ± 0.04	0.7 ± 0.1	1.131 ± 0.005	19.8 ± 0.1
15	0.36 ± 0.02	4.1 ± 0.3	0.68 ± 0.02	16.0 ± 0.3
25	0.70 ± 0.06	3.8 ± 0.3	0.40 ± 0.07	10.8 ± 0.9
50	1.04 ± 0.05	0.99 ± 0.09	0.20 ± 0.06	4 ± 1
75	-	-	1.36 ± 0.04	3.5 ± 0.1
100	-	-	1.49 ± 0.03	5.8 ± 0.2

4.2. $Ni - mnt_{0.01\%}^{prot}$

4.2.1. ESE-detected Spectra

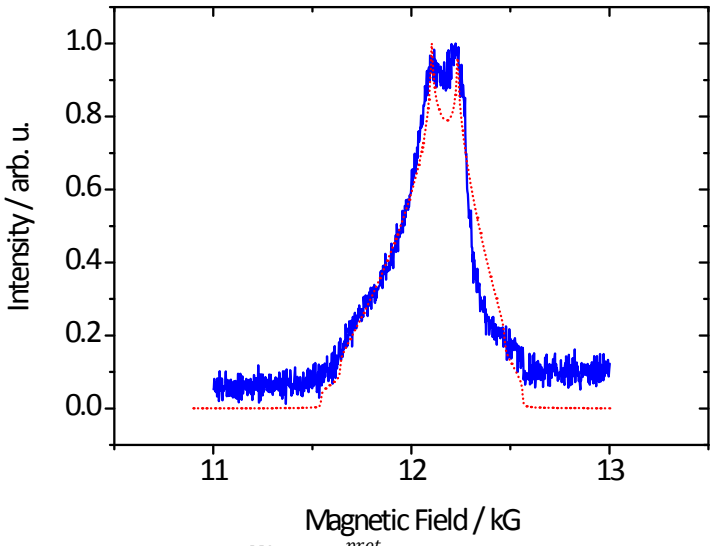

Figure S10: ESE detected EPR-spectrum of $Ni - mnt_{0.01\%}^{prot}$ at 7 K (blue, solid line) and simulation (red, broken line; parameters see Table 10).

Table S10: Simulation parameters for ESE-detected EPR spectra of $\mathrm{Ni\text{ - }mnt}_{0.01\%}^{prot}$ at 7 K. Two S = ½ spin systems were used in the simulation as well as a slight orientation effect with a preferential orientation of the molecules along the g_y-axis.

System	g_z	g_y	g_x	lwpp	weight
1	2.166 ± 0.001	2.0440 ± 0.0005	1.991 ± 0.001	[0.2 0.3]	1
2	2.148 ± 0.001	2.0660 ± 0.0005	2.005 ± 0.001	[0.2 0.3]	0.9

4.2.2. Temperature Dependence of Electron Spin Relaxation

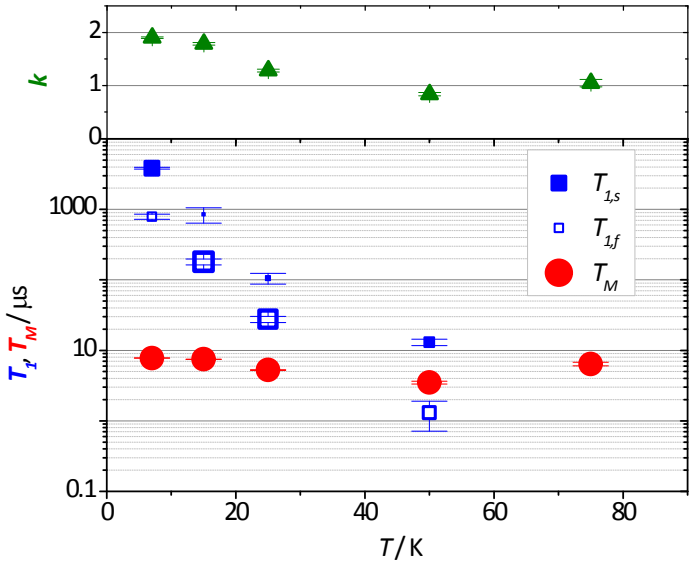

Figure S11: Temperature dependence of relaxation times in $^{\mathrm{Ni\text{ - }mnt}}_{0.01\%}^{prot}$, recorded at 12209 G.

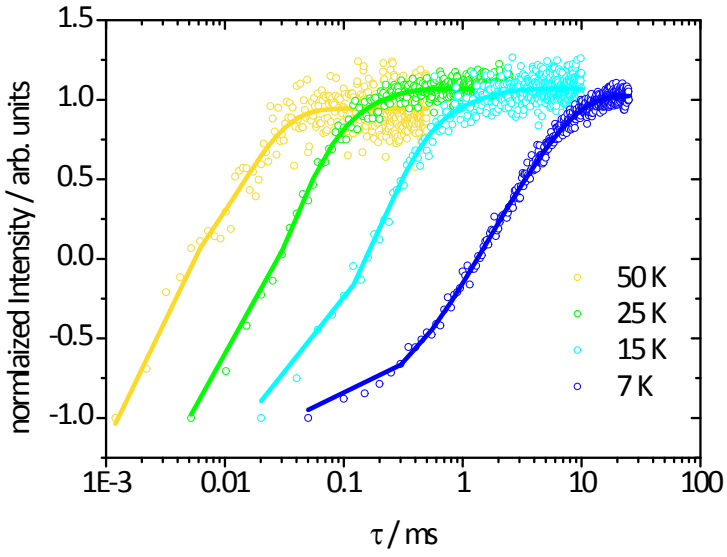

Figure S12: Inversion recovery data (open symbols) and mono-/biexponential fits (solid lines) of $^{\mathrm{Ni\text{ - }mnt}}_{0.01\%}^{prot}$ measured at 12209 G, 7-50 K. Fit parameters are given in Table 11.

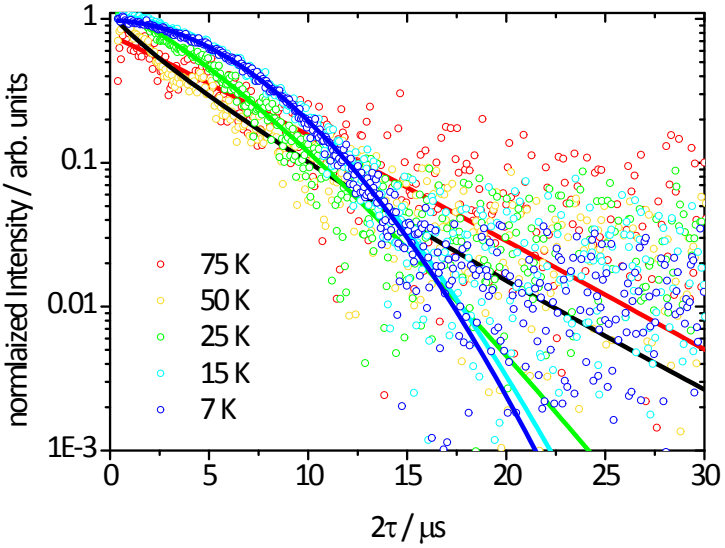

Figure S13: Hahn echo data (open circles) and stretched exponential fit functions (solid lines) of ^{Ni} - $mnt^{prot}_{0.01\%}$ measured at 12209 G, 7-75 K. Fit parameters are given in Table 12.

Table S11: Parameters of bi-/monoexponential fit functions for inversion recovery experiments of ^{Ni} - $mnt^{prot}_{0.01\%}$ measured at 12209 G, 7-50 K.

T / K	A_f	$T_{1,f}$ / µs	A_s	$T_{1,s}$ / µs
7	-0.80 ± 0.04	788 ± 64	-1.24 ± 0.04	3827 ± 115
15	-1.8 ± 0.1	180 ± 18	-0.4 ± 0.1	844 ± 206
25	-1.9 ± 0.1	28 ± 3	-0.5 ± 0.2	105 ± 19
50	-1.8 ± 0.7	1.3 ± 0.6	-1.4 ± 0.2	13 ± 1

Table S12: Parameters of stretched exponential fit functions for Hahn echo experiments of ^{Ni} - $mnt^{prot}_{0.01\%}$ measured at 12209 G, 7-75 K.

T / K	$T_{M,s}$ / µs	k
7	7.78 ± 0.03	1.90 ± 0.02
15	7.49 ± 0.04	1.78 ± 0.02
25	5.26 ± 0.07	1.28 ± 0.03
50	3.5 ± 0.2	0.84 ± 0.03
75	6.4 ± 0.4	1.05 ± 0.07

5. References

(1) Schlindwein, S. H.; Bader, K.; Sibold, C.; Frey, W.; Neugebauer, P.; Orlita, M.; van Slageren, J.; Gudat, D. *Inorg. Chem.* **2016**, *55*, 6186 − 6194.

(2) Tkach, I.; Baldansuren, A.; Kalabukhova, E.; Lukin, S.; Sitnikov, A.; Tsvir, A.; Ischenko, M.; Rosentzweig, Y.; Roduner, E. *Appl. Magn. Reson.* **2008**, *35*, 95.

(3) Stoll, S.; Schweiger, A. *J. Magn. Reson.* **2006**, *178*, 42.